

Low-frequency phase locking in high-inductance superconducting nanowires

R. H. Hadfield, A. J. Miller, S. W. Nam, R. L. Kautz, and R.E. Schwall

National Institute of Standards and Technology, 325 Broadway, Boulder, Colorado 80305, USA.

(Dated: June 14, 2005)

Niobium nitride nanowires show considerable promise as high-speed single-photon detectors. We report the observation of an anomalous low-frequency (~ 10 MHz) response in long, superconducting NbN nanowires (100 nm wide, 4 nm thick, and 500 μm long). This behavior, although strikingly reminiscent of the ac Josephson effect, can be explained by a relaxation oscillation resulting from the high kinetic inductance of the type II nanowire. We simulate all of the observed effects using a simple resistive-hotspot/series-inductor model. The voltage pulses observed are indistinguishable from the pulses induced by visible photons, and our observations suggest noise-induced relaxation oscillations as a primary mechanism for the dark counts in photon detectors.

PACS numbers: 74.76.Db, 85.25.-j

Work of the U.S. Government, not subject to U.S. copyright.

The high-speed (gigahertz) photoresponse of superconducting nanowires of ultrathin NbN films was first identified by Gol'tsman *et al.*,¹ and longer meander wires have been shown to yield quantum efficiencies of up to 20% at visible wavelengths.^{2,3} These properties make superconducting nanowires highly attractive for fast single-photon counting, particularly at telecommunications wavelengths. A simple description of the photoresponse runs as follows: when a photon hits a wire biased just below its critical current, a hotspot of excited quasiparticles is momentarily formed. This perturbation of the superconducting state leads to a high-speed voltage pulse that propagates along a 50 Ω transmission line to a high-speed amplifier, allowing the pulse to be observed on an oscilloscope.

In this Letter we report the observation of pulses in long NbN nanowires biased by a current source with dc and rf components. The pulses are virtually identical to those induced by optical photons but are explained by a simple relaxation-oscillator model that may also apply to photon detection. The model explains both the dc current-voltage ($\bar{I}-\bar{V}$) characteristic of the wire and the presence of constant-voltage steps induced by the rf drive.

In our experiment, the nanowire (embedded on-chip in a 50 Ω coplanar waveguide) is mounted in a Gifford-McMahon cryocooler (base temperature 2.9 K) and connected to room temperature by a 50 Ω semi-rigid coax. A 50 Ω shunt is placed in parallel with the device, and the voltage across the parallel combination is recorded by a digital voltmeter. A dc bias plus a low-frequency (13.4 MHz) rf excitation are applied through the dc arm of a bias tee. High-speed voltage pulses are read out from the ac arm of the bias tee on an 8 GHz digital storage oscilloscope.

Figure 1 shows the $\bar{I}-\bar{V}$ curve of the nanowire both (a) without and (b) with the 13.4 MHz drive. The rf-induced steps in (b) might be mistaken for the Shapiro steps of a Josephson junction, except that the interval between steps is much larger than the voltage quantum $\Delta V = hf/2e = 28$ nV for a junction driven at $f = 13.4$ MHz. Indeed, an explanation in terms of the

Josephson effect would require a series array of 5000 junctions acting coherently. Given the improbability of this scenario, we advocate an alternate explanation based on the hotspot/inductor model illustrated in Fig. 2. Here, the nanowire is represented by an inductance L , representing the wire's kinetic inductance, in series with a current-activated hotspot. The hotspot switches from superconducting to normal when the current exceeds the critical current I_c and becomes superconducting again when the current is reduced below the return current I_r . The physical basis for such hysteretic hotspots has been explored by Skocpol *et al.*⁴

When the nanowire is driven by a dc source $I_s = I_0$ with a small source impedance R_s , we see from Fig. 2 that the load line intersects a branch of the hotspot $I-V_h$ characteristic only for $|I_0| \leq I_c$ or $|I_0| \geq I_r(1 + R_n/R_s)$. At currents between these limits, $I_r(1 + R_n/R_s) < |I_0| < I_c$, the superconducting and normal states are both unstable, and the nanowire displays relaxation oscillations in which it circles around the hysteresis loop, alternating between these states. In simulations, when I_0 first exceeds I_c the voltage suddenly jumps from 0 to 0.25 mV as relaxation oscillations begin. This jump is shown in Fig. 1(a) as a dotted segment of the theory curve and is mimicked by a sparsity of points in the experimental curve. Above $\bar{V} = 0.25$ mV, the oscillations increase in frequency with increasing voltage.

When the nanowire is also driven by an rf source, $I_s = I_0 + I_1 \sin(2\pi ft)$, we obtain a step structure in the $\bar{I}-\bar{V}$ curve, as shown in Fig. 1(b). Although these steps are similar to Shapiro steps, with a voltage spacing that increases in proportion to the frequency f , they result from phase lock between the rf drive and relaxation oscillations, not Josephson oscillations. In the nanowire, a step of order n results when the difference in the number of positive and negative relaxation oscillations is exactly n in each drive cycle. Nonetheless, the range of nanowire current ΔI_n over which phase lock persists on the n th step follows a pattern very close to that of Shapiro steps in an overdamped Josephson junction.⁵ As shown in Fig. 3, a similar pattern of ΔI_n as a function of rf am-

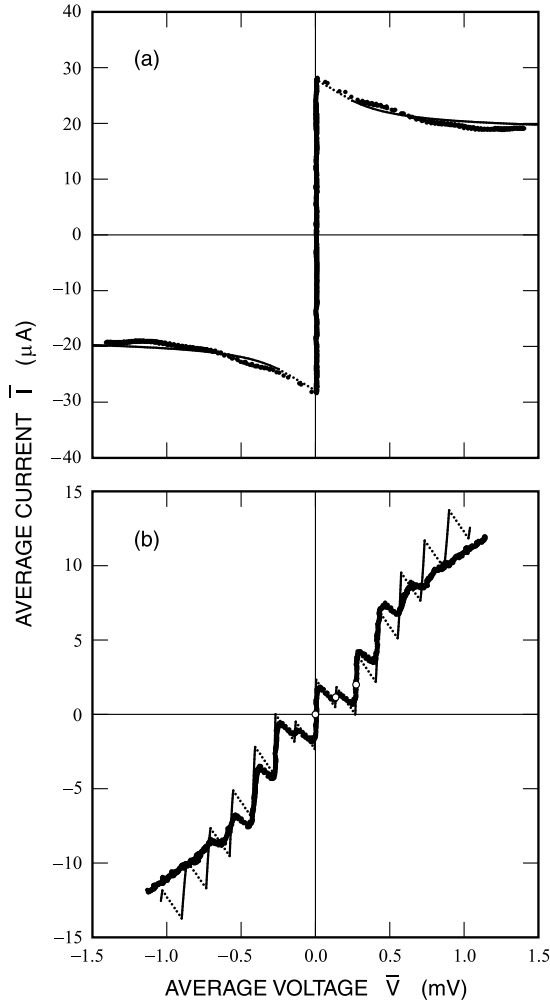


FIG. 1: Current-voltage characteristics of a NbN nanowire (a) in the absence of an rf bias and (b) when driven at 13.4 MHz. The nanowire is a meander $w = 100$ nm wide, $s = 4$ nm thick, and $\ell = 500$ μm long and is cooled to 2.9 K. Experimental points are shown as bold dots, and simulations as narrow solid lines in stable regions and dotted lines in unstable regions. In (b) the simulated rf amplitude is $I_1 = 39$ μA .

plitude is reproduced for the $n = 0, 1$ and 2 steps both in the nanowire experiment and in the hotspot/inductor model. However, despite such similarities, the nanowire steps are not fundamentally quantized like Shapiro steps.

The nature of the relaxation oscillations is revealed in Fig. 4, where we show experimental and theoretical voltage waveforms for bias points on the $n = 0, 1$ and 2 steps. These bias points are indicated by open circles in Fig. 1(b). To facilitate comparison, the average voltage and the Fourier component at the drive frequency were removed from all waveforms. In Fig. 4, each relaxation oscillation appears as a voltage spike with a sharp rise or fall followed by a more gradual decay. Thus, we see that the $n = 0$ step is represented by one positive and one negative spike, while the $n = 1$ step has two positive spikes and one negative spike, and the $n = 2$ step has two

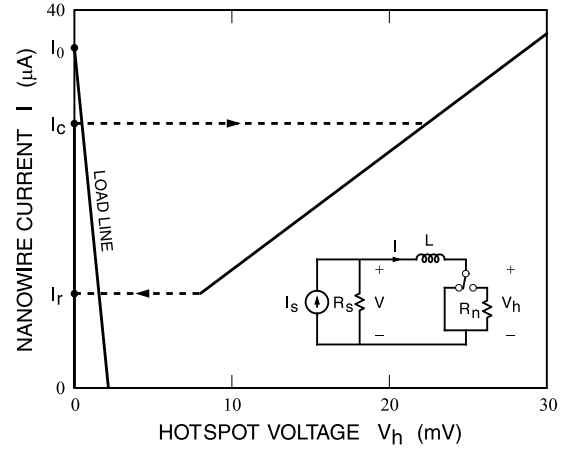


FIG. 2: Model of a superconducting nanowire including a hotspot. The model parameters are $I_c = 28$ μA , $I_r = 10$ μA , $R_n = 800$ Ω , $L = 500$ nH, and $R_s = 60$ Ω .

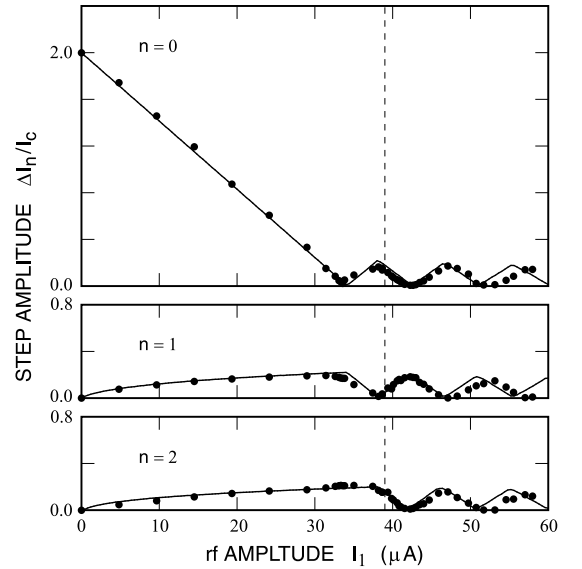


FIG. 3: Current amplitude of rf-induced steps of order $n = 0, 1$, and 2 as a function of rf amplitude. Bold dots show experimental results and lines show simulations for the model parameters given in Fig. 2. The dashed vertical line corresponds to the rf amplitude $I_1 = 39$ μA of Figs. 1(b) and 3.

positive spikes. The negative spikes occur because the rf amplitude $I_1 = 39$ μA is large enough that I not only exceeds I_c on the positive half cycle of the rf drive but falls below $-I_c$ on the negative half cycle. At somewhat lower rf amplitudes, corresponding to the first lobe of each step in Fig. 3, the negative pulses are absent and waveforms on the $n = 0$ and 1 steps have 0 and 1 positive pulses, respectively.

The sharp rise at the leading edge of a positive voltage spike results when the hotspot switches from the superconducting to the normal state and the current I through the inductor begins to decay with a relaxation time $\tau_r = L/(R_n + R_s) = 0.58$ ns. Then, when I falls be-

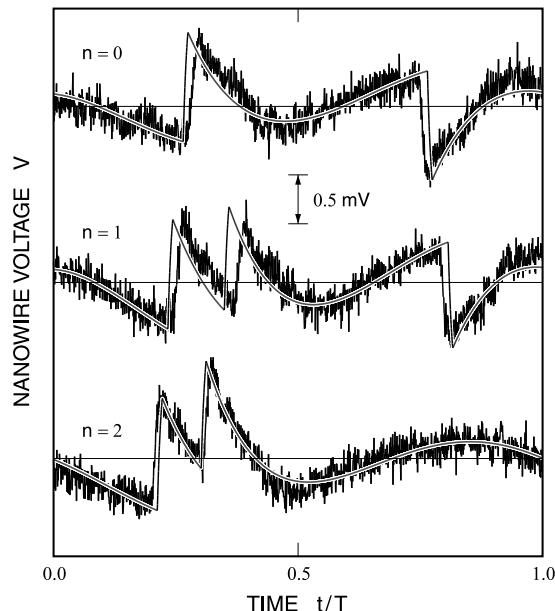


FIG. 4: Voltage waveforms of the rf-biased nanowire on the $n = 0, 1$ and 2 steps plotted over one drive period, $T = 1/f = 74.6$ ns. Simulations, shown by narrow lines, are for the three bias points indicated by open circles in Fig. 1(b) with $I_0 = 0, 3.4$, and $6.9 \mu\text{A}$ and $I_1 = 39 \mu\text{A}$. The average voltage and the Fourier component at the drive frequency were removed from each curve. The experimental curves were shifted in time and scaled by a common factor to fit the theory curves.

low I_r , the hotspot returns to the superconducting state and V begins to fall again while I rises with the somewhat longer relaxation time $\tau_f = L/R_s = 8.3$ ns. Thus, the asymmetry of the voltage spikes is well explained by the inductor/hotspot model.

Most of the various model parameters listed in Fig. 2 were adjusted to obtain a good fit between theory and the experimental data presented in Figs. 1, 3, and 4. Thus, while R_s and I_c were measured directly, we must ask whether other parameters make physical sense. In particular, could the nanowire have a kinetic inductance of $L = 500$ nH? In the limit that the film thickness s is much less than the London penetration depth λ , the kinetic inductance of a wire of width w and length ℓ is $L = \mu_0 \lambda^2 \ell / ws$. For $L = 500$ nH and the measured dimensions of the nanowire, we find $\lambda = \sqrt{wsL/\mu_0 \ell} = 560$ nm. This value is larger than the 200 nm penetration depth

of bulk NbN, but it is well within the range expected for thin films.

Can the hotspot/inductor model be applied to photon-induced voltage pulses as well as the current-induced pulses considered here? A key to producing pulses with our model is the small value of the shunt resistance R_s . If R_s is too large, then the load line will intersect the normal branch of the hotspot characteristic and the nanowire will switch permanently to the normal state rather than follow the hysteresis loop. However, a small shunt need only be present for the time required for the inductor current to decay below I_r and allow the hotspot to reset to the superconducting state, typically about 1 ns. Thus, whenever the nanowire is connected to a 50Ω line more than about 10 cm long, excursions into the normal state will lead to voltage pulses regardless of the dc shunt resistance. Thus, we expect our model to apply to a wide range of situations with large inductance, whether the hotspot is induced by the current exceeding I_c or by photons.

The hotspot/inductor model may not apply to the original photoresponse experiments of Gol'tsman *et al.*¹ which used a short nanowire with small inductance. However, more recent experiments with long nanowires are probably limited in response time by kinetic inductance rather than the internal dynamics of the hotspot. For the sample studied here, this idea is bolstered by the fact that the voltage pulses induced by photons are indistinguishable those induced by current. From this we conclude that both types of pulse result from a single pass along similar hysteresis loops, with the hotspot generated at the point of photon absorption in one case and at a weak spot in the nanowire in the other case.

Finally, the hotspot/inductor model suggests an explanation for the exponential increase in dark counts observed in photon detectors biased very close to I_c .³ These dark counts may be due not to photons from environmental black body radiation, but to current noise that occasionally pushes the bias above I_c , initiating a relaxation oscillation. If so, dark counts might be reduced by including appropriate filters in the bias leads.

This work was funded in part by BBN Technologies. The authors thank R. Sobolewski and G. Gol'tsman for providing the nanowire devices. We also thank K. Berggren, Y. Chong, E. Dauler, A. Kerman, A. Pearlman, H. Rogalla, R. Sobolewski, and J. Yang for insightful discussions.

¹ G. N. Gol'tsman, O. Okunev, G. Chulkova, A. Lipatov, A. Semenov, K. Smirnov, B. Voronov, A. Dzardanov, C. Williams, R. Sobolewski, Appl. Phys. Lett. **79** 705 (2001).

² A. Verevkin, J. Zhang, R. Sobolewski, A. Lipatov, O. Okunev, G. Chulkova, A. Korneev, K. Smirov, G. N. Gol'tsman, and A. Semenov, Appl. Phys. Lett. **80** 4687 (2002).

³ A. Korneev, P. Kouminov, V. Matvienko, G. Chulkova, K.

Smirnov, B. Voronov, G. N. Gol'tsman, M. Currie, W. Lo, K. Wilsher, J. Zhang, W. Słysz, A. Pearlman, A. Verevkin, and R. Sobolewski, J. Appl. Phys. **84**, 5338 (2004).

⁴ W. J. Skocpol, M. R. Beasley, and M. Tinkham, J. Appl. Phys. **45**, 4054 (1974).

⁵ M. J. Renne and D. Polder, Revue de Physique Appliquée **9**, 25 (1974).